

P₂S₂-Bridged Binuclear Metal Carbonyls from Dimerization of Coordinated Thiophosphoryl Groups: A Theoretical Study

Zhong Zhang,^{*a} Zuqing Chen,^a Zhipeng Yang,^a Jianping Wang,^a Liang Pu,^a Lingzhi Zhao,^{*b} R. Bruce King^{*c}

^aCollege of Chemistry & Pharmacy, Northwest A&F University, Yangling, Shaanxi 712100, P. R. China

^bSCNU Qingyuan Institute of Science and Technology Innovation Co., Ltd., Qingyuan 511517, China

^cDepartment of Chemistry and Center for Computational Chemistry, University of Georgia, Athens, Georgia 30602, USA

Supporting Information:

Figure S1. Optimized other mononuclear PS complexes and dimers.

Figure S2. Molecular orbital (unit in a. u.) of **Mn**.

Figure S3. Comparing the molecular orbitals of N₂S₂ P₂S₂ and **dMn**.

Figure S4. Optimized transition states.

Table S1. Dimerization energies (in kcal/mol) with different methods.

Table S2. Dimerization energies (in kcal/mol).

Table S3. Wiberg bond indexes and natural charges of monomers.

Table S4. Wiberg bond indexes and natural charges of dimers.

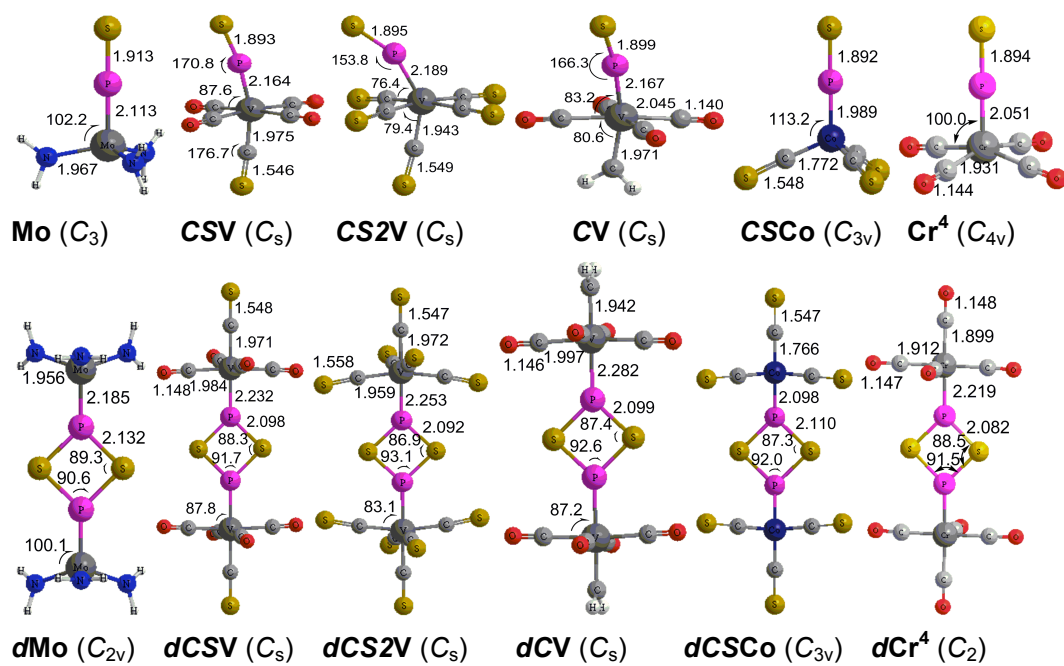


Fig. S1. Optimized other mononuclear PS complexes and dimers showing selected bond distances (Å) and bond angles (degrees).

The new Double-Hybrid Density Functional (DHDF), which considers electron correlation by an additional E_c term derived from the MP2 method, are expected to give more reliable results in prediction of reaction energies.¹ Two such DHDF methods, namely pPB95² and B97-M³, were used with aug-cc-pVTZ basis sets herein for single point energy calculations of the optimized structures. The long range dispersion effect D4⁴ method is included in the pPB95 functional. These calculations were performed with the ORCA 4.2 program.^{5,6}

TableS1. Dimerization energies (in kcal/mol) with different methods.

	ΔE	ΔE^a	ΔE^b	ΔE^c
<i>dV</i>	-6.1	-5.5	-13.0	-15.7
<i>dCr</i>	-43.0	-26.8	-49.2	-43.4
<i>dMn</i>	-24.6	-18.7	-18.4	-34.1
<i>dFe</i>	-28.0	-4.6	-39.5	-27.6
<i>dCo</i>	-3.7	-2.2	16.6	-12.1

^a: Single point energies at CCSD/cc-pVDZ//M06L/cc-pVTZ level.

^b: Single point energies at pPB95-D4/aug-cc-pVTZ//M06L/cc-pVTZ level.

^c: Single point energies at B97-M/aug-cc-pVTZ//M06L/cc-pVTZ level.

Additional dimerization energies were determined at three different levels (see Table S2). The ideal benchmark energies are obtained by the CCSD(T)/cc-pVTZ//M06L/cc-pVTZ method. However, our computational resources are limited for CCSD/cc-pVDZ//M06L/cc-pVTZ calculations. For the closed shell systems (***dV***, ***dMn***, ***dCo***), the CCSD/cc-pVDZ//M06L/cc-pVTZ energies match well our M06L/cc-pVTZ results with the largest difference being 5.9 kcal/mol. However, for the open shell systems (***Fe*** and ***Cr***), the CCSD/cc-pVDZ//M06L/cc-pVTZ single point calculation gives very bad results with major energy differences up to 23.4 kcal/mol (***dFe***) owing to the small basis sets limit as well as lacking of triple excitation. The robust pPB95-D3 method was obtained from the main group GMTKN30 Database, but also provided good results with transition metal carbonyls.² However, the MPN is not a self-consistent method, thus giving fluctuating ΔE s, especially the ΔE of 16.6 kcal/mol for ***dCo***. We cannot say that the pPB95-D4/aug-cc-pVTZ//M06L/cc-pVTZ is adequate, since it gives a positive ΔE for ***dCo***, when all of the other methods give a negative ΔE for this system (Table S1). The B97-M/aug-cc-pVTZ//M06L/cc-pVTZ results are generally larger than those from M06L and CCSD. However, most of calculated ΔE s for ***dCr***, ***dMn*** and ***dFe*** are larger than -18.7 kcal/mol, indicating clearly thermodynamically favored dimerizations (see Table S2).

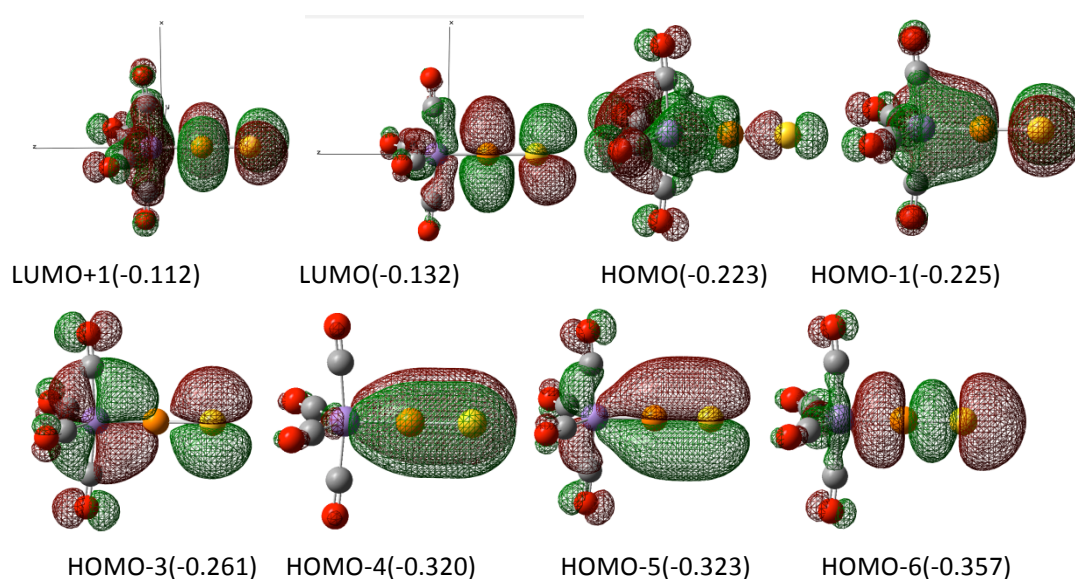


Figure S2. Molecular orbitals of Mn^4 with energies in atomic units..

The perpendicular HOMO-1 and in-planar HOMO-3 orbitals indicate two Mn–P π bonds. However, the two Mn–P π bonding orbitals are not degenerate in energy. Thus the orbital energy of HOMO-1 is -0.225a.u. , as compared with -0.362 a. u. for HOMO-3. The more efficient overlap between the $\text{Mn}(\text{CO})_4$ and PS fragments leads to stabilization of the MO. Therefore, HOMO-3 has a more negative energy than HOMO-1 because of its stronger Mn–P overlap.

The HOMO-4 and HOMO-5 are nearly degenerate in energy, since these orbitals are mainly similar P–S bonding orbitals.

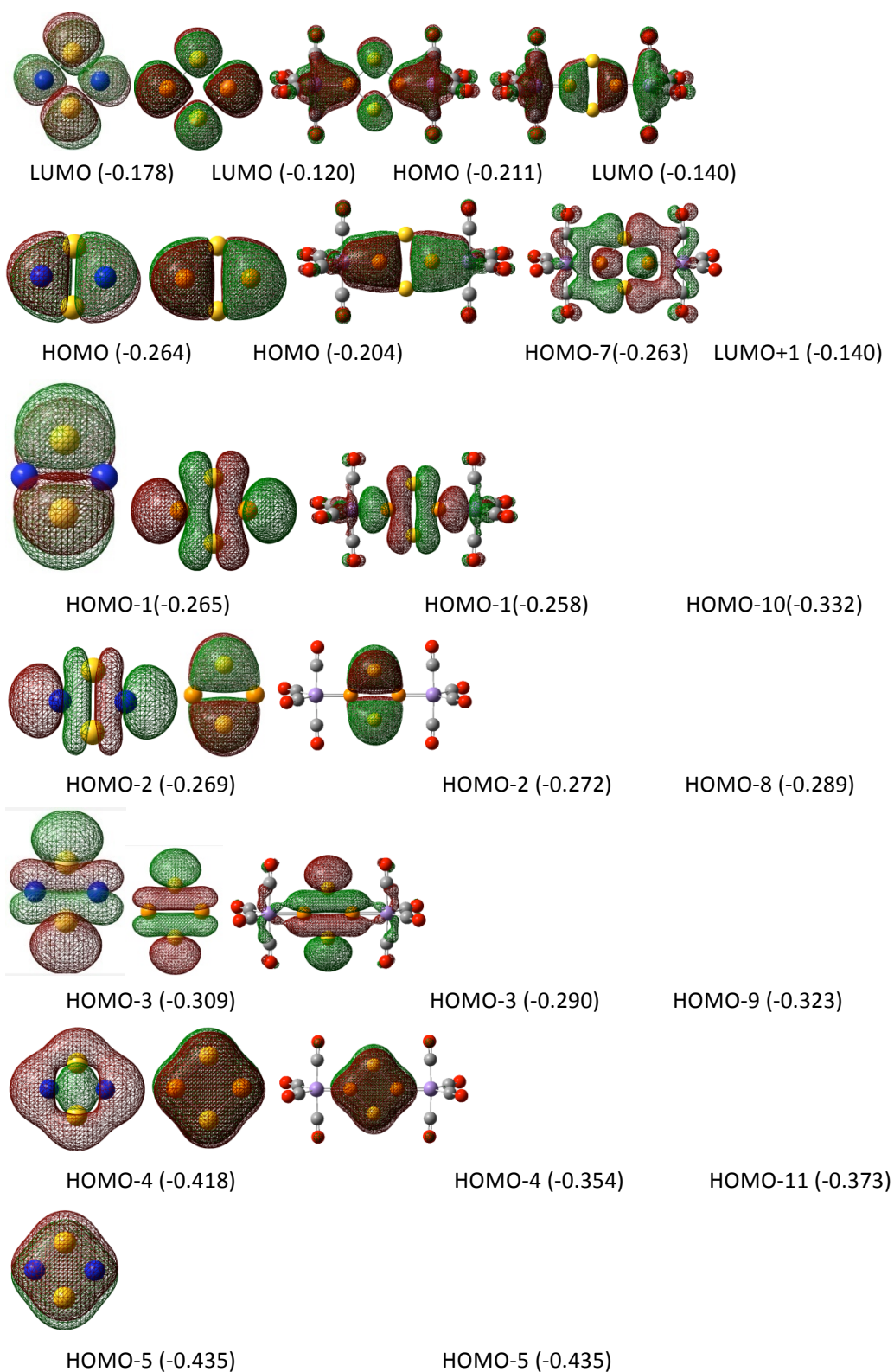
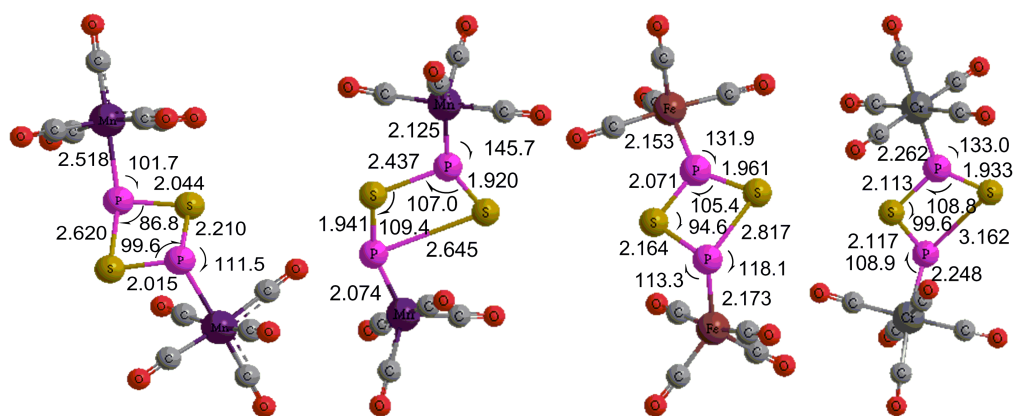


Figure S3. Comparison of the molecular orbitals of N_2S_2 , P_2S_2 , and dMn .



$d\text{Mn}^5\text{-TS}$ (2.6, -3.8) $d\text{Mn}^4\text{-TS}$ (25.7, 16.2) $d\text{Fe}^4\text{-TS}$ (-12.4, -13.7) $d\text{Cr}^5\text{-TS}$ (-11.7, -13.7)
Figure S4. Optimized transition states. The activation free energies (in kcal/mol) at DLPNO-CCSD(T)/cc-pVTZ//M06L/cc-pVTZ and M06L/cc-pVTZ level, respectively.

Table S2. Dimerization energies (in kcal/mol).

	<i>dMo</i>	<i>dV</i>	<i>dCSV</i>	<i>dCS2V</i>	<i>dCV</i>	<i>dCo</i>	<i>dCSCo</i>	<i>dMn</i>	<i>dFe</i>
ΔE	-3.4	-6.1	-7.8	-11.8	-20.7	-3.7	-14.2	-24.6	-28.0
ΔH	-2.1	-6.5	-10.1	-13.3	-20.9	-2.9	-13.3	-23.5	-27.4
ΔG	8.9	7.3	14.6	9.1	-8.3	8.3	-0.1	-10.0	-12.4

Table S3. Wiberg bond indexes and natural charges of the monomers.

WBI	Mo	V5	Co3	Mn4	Cr5	Cr4	Fe4	Fe3	Mn5	V6	Co4
MP	2.03	<u>1.67</u>	<u>1.59</u>	<u>1.57</u>	1.01	1.67	1.06	1.53	<u>0.71</u>	0.70	<u>0.76</u>
PS	1.66	<u>1.90</u>	<u>1.94</u>	<u>1.94</u>	1.87	1.89	1.78	1.90	<u>1.99</u>	1.93	<u>1.98</u>
MS	0.43	0.33	0.33	<u>0.31</u>	0.16	0.34	0.18	0.29	<u>0.12</u>	0.20	<u>0.16</u>
<i>qM</i>	0.26	-3.08	-1.69	-2.57	-2.96	-2.38	-2.15	-1.60	-2.72	-2.94	-1.75
<i>qP</i>	0.72	<u>1.06</u>	<u>0.87</u>	<u>1.00</u>	0.78	1.01	0.66	0.82	<u>0.53</u>	0.57	<u>0.57</u>
<i>qS</i>	-0.37	<u>-0.26</u>	<u>-0.25</u>	<u>-0.25</u>	-0.26	-0.28	-0.27	-0.26	<u>-0.32</u>	-0.28	<u>-0.30</u>
<i>qPS</i>	0.35	0.80	0.62	0.74	0.52	0.73	0.39	0.56	0.21	0.29	0.27

Table S4. Wiberg bond indices and natural charges of the dimers.

WBI	<i>dMo</i>	<i>dV6</i>	<i>dV5</i>	<i>dMn5</i>	<i>dMn4</i>	<i>dCr5</i>	<i>dCr4</i>	<i>dFe4</i>	<i>dFe3</i>	<i>dCo4</i>	<i>dCo3</i>
MP	1.66	<u>0.58</u>	<u>1.47</u>	<u>0.67</u>	<u>1.35</u>	0.86	1.03	0.85	1.20	<u>0.70</u>	<u>1.27</u>
PS	0.90	<u>1.02</u>	<u>1.00</u>	<u>0.99</u>	<u>0.99</u>	1.07	1.05	1.05	1.01	<u>1.00</u>	<u>1.00</u>
MS	0.15	0.05	0.10	0.04	0.09	0.07	0.08	0.07	0.10	0.05	0.09
PP	0.03	0.05	0.04	0.03	0.05	0.25	0.19	0.21	0.10	0.04	0.04
SS	0.14	0.12	0.16	0.07	0.14	0.17	0.18	0.15	0.16	0.09	0.15
<i>qM</i>	0.34	-2.84	-2.89	-2.65	-2.35	-2.93	-2.04	-2.11	-1.44	-1.70	-1.42
<i>qP</i>	0.51	<u>0.51</u>	<u>0.87</u>	<u>0.49</u>	<u>0.73</u>	0.68	0.59	0.62	0.60	<u>0.54</u>	<u>0.65</u>
<i>qS</i>	-0.29	<u>-0.27</u>	<u>-0.18</u>	<u>-0.34</u>	<u>-0.18</u>	-0.15	-0.13	-0.17	-0.16	<u>-0.31</u>	<u>-0.21</u>
<i>qPS</i>	0.23	0.24	0.70	0.05	0.55	0.53	0.46	0.45	0.44	0.23	0.45

References

- (1) I. Y. Zhang and X. Xu, *A New-Generation Density Functional-Towards Chemical Accuracy for Chemistry of Main Group Elements*. Springer, **2013**.
- (2) L. Goerigk and S. Grimme, *J. Chem. Theory Comput.* **2011**, *7*, 291.
- (3) L. Goerigk and S. Grimme, *Phys. Chem. Chem. Phys.* **2011**, *13*, 6670.
- (4) E. Caldeweyher, S. Ehlert, A. Hansen, H. Neugebauer, S. Spicher, C. Bannwarth and S. Grimme, *J. Chem. Phys.* **2019**, *150*, 154122.
- (5) Neese, F. "The ORCA program system" *Wiley Interdisciplinary Reviews: Computational Molecular Science*, **2012**, *2*, 73–78.
- (6) F. Neese, "Software update: the ORCA program system, version 4.0" *Wiley Interdisciplinary Reviews: Computational Molecular Science*, **2017**, *8*, 1327.